Multipactor Effect in a Parallel-Plate Waveguide Partially Filled with Magnetized Ferrite

D. González-Iglesias, B. Gimeno, *Member, IEEE*, V. E. Boria, *Senior Member, IEEE*, Á. Gómez, *Member, IEEE*, A. Vegas, *Member, IEEE*

***Abstract*—The aim of this paper is the analysis of the multipactor effect in a parallel-plate waveguide when a ferrite slab, transversally magnetized by a static magnetic field parallel to the waveguide walls, is present. Employing an in-house developed code, numerical simulations are performed in order to predict the multipactor RF voltage threshold in such a ferrite-loaded waveguide. Variations of the ferrite magnetization field strength and the ferrite slab height are analyzed. Effective electron trajectories are also shown for a better understanding of the breakdown phenomenon, finding different multipactor regimes.**

***Index Terms*—Multipactor effect, RF breakdown, parallel-plate waveguide, ferrite components.**

I. Introduction

Multipactor is a high-power radio frequency (RF) electromagnetic field phenomenon that appears on devices operating under vacuum conditions [1]. It is present in a wide range of different scenarios, such as passive components of satellite communication payloads, travelling-wave tubes or particle accelerators. In vacuum environment, free electrons inside a microwave device are accelerated by the RF electric field, impacting against its metallic walls. If the electron impact energy is high enough, one or more secondary electrons may be released from the surface. When some resonant conditions are satisfied, secondary electrons get synchronized with the RF electric field, and the electron population inside the device grows exponentially leading to a multipactor discharge. The onset of a multipactor discharge in a device has negative effects that degrade its performance.

Multipactor research lines are aimed to study and characterize the phenomenon in order to predict under which conditions it will appear [2]-[6]. Some RF devices, such as filters, gyrators, circulators, isolators, and phase-shifters, use ferrite components which are magnetized by means of an external permanent field [7]-[13]. The presence of such an external magnetic field is expected to perturb the classical resonant multipactor regimes [14]-[16]. Therefore, previous multipactor studies are not useful to predict the discharge on devices involving ferrites. However, to the authors' knowledge, very few contributions about multipactor on ferrite materials can be found [17].

D. González-Iglesias and B. Gimeno are with Depto. Física Aplicada-ICMUV, Universidad de Valencia, Spain (email: daniel.gonzalez-iglesias@uv.es; benito.gimeno@uv.es)

V. E. Boria is with Depto. Comunicaciones-iTEAM, Universidad Politécnica de Valencia, Spain (email: vboria@dcom.upv.es)

Á. Gómez and A. Vegas are with Depto. Ingeniería de Comunicaciones, Universidad de Cantabria, Spain (email: alvaro.gomez@unican.es; angel.vegas@unican.es)

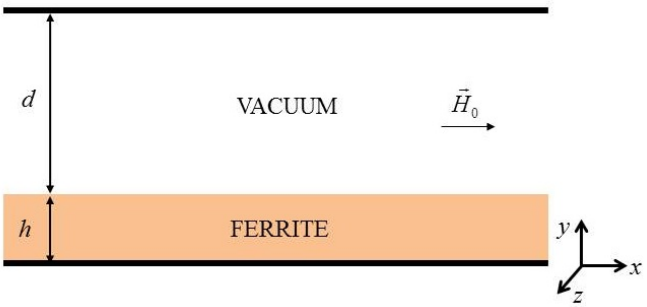

Fig. 1. Parallel-plate waveguide partially filled with a ferrite slab transversally magnetized by a static magnetic field.

In this paper, we are interested on the multipactor analysis of a metallic parallel-plate waveguide partially filled with a ferrite slab, placed just above the metal bottom wall, and transversally magnetized by a static (DC) magnetic field parallel to the waveguide walls (see Fig. 1). The present study might be used for a preliminary analysis of multipactor phenomenon in the aforementioned devices containing ferrite, specially, some kind of isolators (resonance isolator) and phase shifters (nonreciprocal latching phase shifters) [18]-[20]. The paper is organized as follows. First, in section II, the theoretical model employed for the simulations is discussed. Next, in section III, some multipactor susceptibility charts and the effects of the variation of some fundamental parameters, such as ferrite height and ferrite magnetization field strength, are introduced. Finally, in section IV, the conclusions of the paper are outlined.

II. Theory

In this work, the magnetization field is oriented along the x axis, parallel to the the waveguide walls. The waveguide structure under study is shown in Fig. 1, being d the vacuum gap length, h the ferrite slab height and ε_r its relative dielectric permittivity. The RF electromagnetic field is assumed to propagate along the positive direction of the z axis. For the sake of simplicity, in this model the waveguide is supposed to be infinite in the z and x directions. In this work, an $e^{j\omega t}$ time–dependance is implicitly assumed, ω being the angular frequency and t the time.

In any actual microwave device involving ferrites, an external static magnetic field H_0 must be applied in order to magnetize the ferrite. As a first approach, this external magnetic field is assumed to be uniform over the entire waveguide. When the

applied magnetic field is strong enough, the ferrite reaches the saturation magnetization and behaves like a magnetic medium, described by a gyrotropic permeability tensor $\overleftrightarrow{\mu}$ (see formula 9.26 in [21]).

The RF electromagnetic fields supported by a waveguide with the aforementioned characteristics can be obtained analytically. In this situation two family of electromagnetic field modes are found: TM^z ($H_z = 0$) and TE^z ($E_z = 0$). Following the same procedure outlined in [21], it can be analytically demonstrated that the TE^z modes have no vertical electric field component along the gap, so they are not suitable to hold a multipactor discharge and, as a consequence, they are not considered in our analysis. Otherwise, the TM^z modes do have vertical electrical component, so they may lead to a multipactor discharge. After imposing the boundary conditions on the significant surface interfaces of the problem, the propagation factor β of the TM^z modes is found by solving numerically the following characteristic equation,

$$\varepsilon_r k_1 \sinh(k_1 d)\, \cos(k_2 h) - k_2 \cosh(k_1 d)\, \sin(k_2 h) = 0$$

where $k_1^2 \equiv \beta^2 - \omega^2 \mu_0\, \varepsilon_0$, $k_2^2 \equiv \omega^2 \mu_0\, \varepsilon_0\, \varepsilon_r - \beta^2$, μ_0 and ε_0 are the magnetic susceptibility and the dielectric permittivity of vacuum, respectively; $f = \omega/(2\pi)$ is the frequency of the RF electromagnetic field. The non-zero TM^z modal field components of the RF electromagnetic field in the vacuum region are given by,

$$E_y(y,z,t) = \frac{V_0\, k_1}{\sinh(k_1\, d)} \cosh[k_1\, ((d+h)-y)]\, \cos(\omega\, t - \beta\, z) \tag{1a}$$

$$E_z(y,z,t) = -\frac{V_0\, k_1^2}{\beta\, \sinh(k_1\, d)} \sinh[k_1\, ((d+h)-y)]\, \sin(\omega\, t - \beta\, z) \tag{1b}$$

$$H_x(y,z,t) = -\frac{\omega\, \varepsilon_0}{\beta} E_y(y,z,t) \tag{1c}$$

where V_0 is the equivalent voltage obtained from the path integration of the RF electric field E_y along the vacuum gap from $y = h$ to $y = d + h$ at $z = 0$ plane and $t = 0$:

$$V_0 = \int_h^{d+h} E_y(y,0,0)dy$$

Note that for the considered TM^z modes the characteristic equation does not depend on the magnetic properties of the ferrite.

In order to obtain the numerical solution for our problem (a parallel plate waveguide partially filled with a ferrite layer), a multipactor simulator code based on the Monte-Carlo algorithm has been developed to compute the RF voltage threshold. The software code, similar to the one described in [22], employs the single effective electron model [23], which consists of tracking the individual trajectories of a certain number of effective electrons. Individual electron trajectories are computed by solving numerically its non-relativistic equation of motion derived from the Lorentz force

$$\vec{F}_L = q(\vec{E} + \vec{v} \times B) = m\vec{a}$$

Here, $q = -e$ is the electron charge, m is the electron mass at rest , $\vec{v}$ is the velocity, $\vec{a}$ is the acceleration, $\vec{E}$ and $\vec{B} = \mu_0 \vec{H}$ are the total electric and total magnetic field (RF and DC contributions) experienced by the electron, respectively.

When one of the effective electrons hits the waveguide walls, secondary electrons may be released from the surface depending on the primary electron impact conditions. The emission of secondary electrons is modelled by the Secondary Electron Yield (SEY) coefficient as formulated in [24]. Initial launching energies for secondary electrons are given by a Gaussian distribution of mean 4 eV and standard deviation 2 eV. The departure angle is selected to be normal to the impacting surface [25].

The current multipactor simulation model includes the space charge effect, that takes into account the Coulombian interaction among electrons [26], [27], as well as the dielectric polarization effect of the ferrite that leads to the presence of a DC electric field, as reported in [27], [28].

III. Simulations

The simulation model previously described in section II is now used to compute the multipactor RF voltage threshold of the ferrite-loaded parallel-plate waveguide shown in Fig. 1. In the considered case, the waveguide walls are made of silver, whose SEY parameters are: first crossover $W_1 = 30$ eV, the maximum SEY coefficient, $\delta_{max} = 2.22$; and the impact kinetic energy for δ_{max}, $W_{max} = 165$ eV. Regarding to the ferrite slab, its relative dielectric permittivity is $\varepsilon_r = 15.5$, the saturation magnetization is $4\pi M_s = 1790$ G, and the SEY parameters are $W_1 = 29$ eV, $\delta_{max} = 2.40$, and $W_{max} = 288$ eV [29].

First of all, we have analyzed the multipactor effect when no external magnetic field is applied to magnetize the ferrite ($H_0 = 0$ Oe, see Fig. 2). We have compared this case with the results presented in [28]-[30], finding good agreement between them. Furthermore, it has also been noticed that in some particular cases the polarization electric field is able to turn the multipactor discharge off, as it was reported in [27] and [28].

Next, we have studied the ferrite magnetization field effect in the multipactor RF voltage threshold. In Fig. 2 multipactor susceptibility charts are shown for several typical values of the magnetization field. It is noticed that the presence of such an external magnetic field really changes the multipactor behavior. First, when the magnetization field is present, the multipactor susceptibility regions are shifted to higher frequency gap values. In fact, the starting frequency gap value for the multipactor zones becomes higher if the magnetization field strength is increased. For $H_0 = 500$ Oe multipactor breakdown does not appear for frequency gap values less than 1.3 GHzmm, while for $H_0 = 1000$ Oe no multipactor discharge is observed below 2.4 GHzmm. Besides, it can be seen in Fig. 2 that there is a frequency gap interval (for both $H_0 = 500$ Oe and $H_0 = 1000$ Oe situations) where the

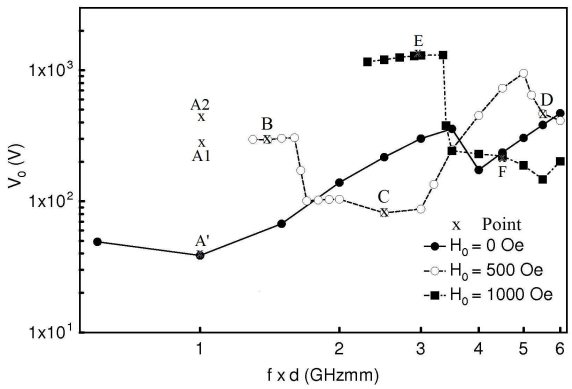

Fig. 2. Multipactor voltage threshold for several values of the external ferrite magnetization field. Waveguide dimensions: $d = 1$ mm and $h = 3$ mm.

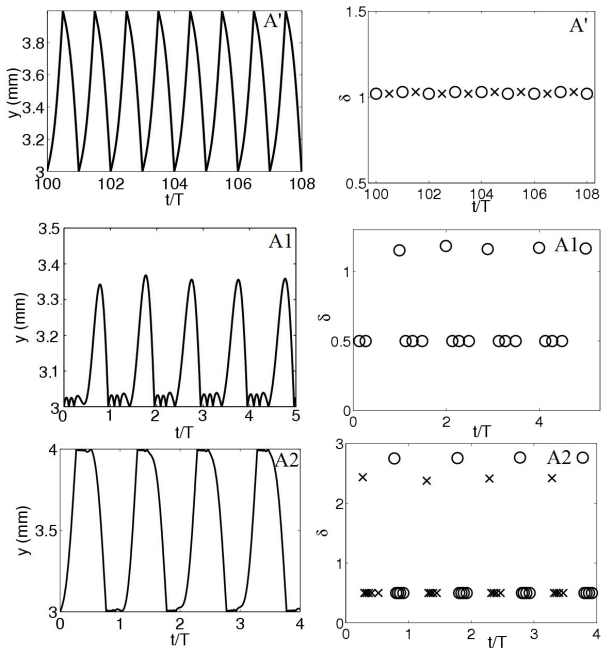

Fig. 3. Vertical coordinate (left column) and SEY impact coefficient (right column) of the effective electron for several points in Fig. 2. SEY coefficient for the impacts with the bottom (upper) wall are denoted by circles (crosses).

multipactor voltage threshold is even less than for the non-magnetized ferrite case. These results are consistent with [14] and [31], wherein it is experimentally demonstrated that the presence of an external DC magnetic field may lead to an enhancement of the multipacting effect for certain values of the external static magnetic field strength.

To have a better understanding of the multipactor behavior, the effective electron trajectories, as well as the SEY coefficient value at the electron impacts, have been plotted for several significant points marked in Fig. 2. Points A1, A2, B, C and D belong to the $H_0 = 500$ Oe case; points E and F to $H_0 = 1000$ Oe, whereas point A' corresponds to the $H_0 = 0$ Oe situation.

First, we are going to compare the effective electron trajectories behavior for the frequency gap value of 1 GHzmm. If we examine the point A' (see Fig. 2 and Fig. 3) it corresponds to the $H_0 = 0$ case, where no external magnetization field is applied. It is observed that the electron takes one semiperiod of the RF signal between successive impacts with the waveguide walls, which corresponds with the well-known classical double surface multipactor of order one. It is also noticed that the mean SEY is slightly above the unity, so the electron population in the device will grow resulting into a multipactor discharge.

In contrast, when the external magnetization field is present, the multipactor effect has not been observed at that frequency gap (1 GHzmm), as it can be seen in Fig. 2. On inspecting point A1 for $H_0 = 500$ Oe (see Fig. 3), it is noticed that the SEY mean value is below one (despite the fact that at some of the impacts the SEY exceeds the unity), implying that there is no discharge. Indeed, as the external DC magnetic field bends the electron trajectories around the magnetic field lines (in our case H_0 is oriented along the x-direction), it will tend to impinge a circular motion in the transverse y-z plane pushing the electron back to the departure wall. This fact destroys the electron resonant trajectories, forcing many low energetic impacts in which the electron is not favored by the RF electric field polarity, and it is pushed back to the departure wall. Both the electron orbit radius and the orbital velocity due to the external DC magnetic field depend on the magnetic field strength, the amplitude of the RF voltage, the ratio between the cyclotron frequency ($f_c = (e\mu_0 H_0)/(2\pi m)$) and the frequency of the RF electromagnetic field [14]. Thus, when the radius of this circular motion is shorter than the waveguide gap value d, the electron will not be able to reach the opposite conductor, as it happens with point A1. Of course, if the RF voltage is increased then the electron will be able to cross the gap, as it is shown for point A2 (see Fig. 3). However, due to the lack of resonance between the electron orbits and the RF electric field, it is found that the SEY mean value remains below the unity, so no multipactor discharge occurs. Points A1 and A2 evidence that it is not only necessary that the electrons impact kinetic energy is enough to release secondaries (SEY values above the unity), but their flight time between successive impacts has to be synchronized with the RF electric field, in order to avoid the electrons being pushed back at the departure instant. In points A1 and A2 the electron flight time between successive impacts is too short (always below the RF semiperiod) to allow a good resonance of the trajectory with the RF electric field. It should be remarked that classical theory of multipactor states that the time between successive impacts must be an odd (even) number of RF semiperiods for double (single) surface multipactor modes. Moreover, we have found that the electron flight time strongly depends on the ratio between the RF frequency and the cyclotron one. Specifically, for a fixed value of the cyclotron frequency, the flight time increases as the RF frequency does. This fact is shown analyzing effective electron trajectories for the points B, C and D corresponding to the $H_0 = 500$ Oe case.

If we focus our attention in point B (see Fig. 2 and Fig. 4), it can be found a multipactor double surface regime of order one, which presents a mean SEY higher than one. Now, the

ratio between the RF and the cyclotron frequencies is higher than for points A1 and A2 and, consequently, the electron flight time has become greater with regard to points A1 and A2. Moreover, the orbital radius has also become greater (note that the RF voltage is very similar to point A1, see Fig. 2). As a consequence, electron is allowed to get resonant with the RF electric field.

Afterwards, for point C (see Fig. 2) single surface multipactor resonance of order two can be observed in Fig. 4, where the SEY is slightly higher than one. In the same way as point B, the increment in the RF frequency related to the cyclotron one allows the electron to increase the flight time impacting over the walls, which gives rise to the appearance of higher order mode resonance. It should also be noticed that in point C the RF multipactor voltage threshold is lower than for point B (see Fig. 2). This result is due to the fact that this single surface resonance does not need the electron to cross the whole gap. Therefore, less energy provided by the RF field is required to produce the discharge.

Next, for point D (see Fig. 2), a single surface regime with order four is shown (the mean SEY is also above the unity). It should be emphasized that the behavior of the RF voltage threshold increases for high values of the frequency gap parameter, in a similar way as it does for the non-magnetized case (see Fig. 2). Despite this, the presence of the external H_0 field allows the presence of single surface multipactor modes and, for nearby frequencies of these resonant modes, the RF voltage threshold shows local minimums as it can be noticed for points C and D.

In Fig. 5 the electron trajectories and the SEY coefficients for the points E and F corresponding to the $H_0 = 1000$ Oe case (see Fig. 2) are plotted. There is a clear correspondence between points E and F, and points B and C of the $H_0 = 500$ Oe case, respectively. Point E shows a double surface multipactor regime of order one (just the same as for point B), whereas for point F a single surface multipactor resonance of order two (the same as for point C) is found. Indeed, the shape of the voltage threshold variation with the frequency gap for the $H_0 = 1000$ Oe case seems to be very similar to the $H_0 = 500$ Oe one, but shifted to higher frequency gap values and voltages. This is because, as mentioned before, the electron flight time is strongly affected by the ratio between the RF frequency and the cyclotron one. Thus, electron flight time determines which resonance order is available at each frequency gap value. Due to this, the same multipactor orders are found for similar values of the ratio between the RF frequency and the cyclotron one.

Finally, the effect of changing the ferrite slab height in the multipactor RF voltage threshold for a fixed value of the gap and the ferrite magnetization field, is analyzed in Fig. 6. As it can be observed, there is a small shift in the voltage threshold, although the general behavior and shape of the multipactor curves remain unchanged for the considered slab height range.

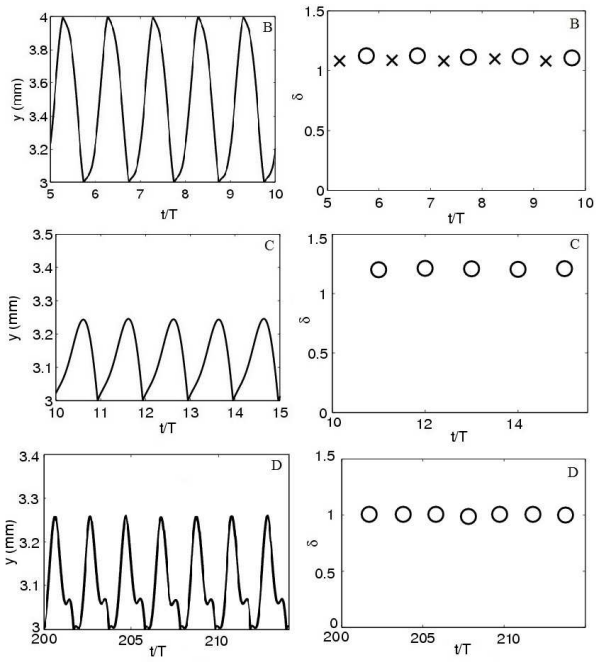

Fig. 4. Vertical coordinate (left column) and SEY impact coefficient (right column) of the effective electron for several points in Fig. 2. SEY coefficient for the impacts with the bottom (upper) wall are denoted by circles (crosses).

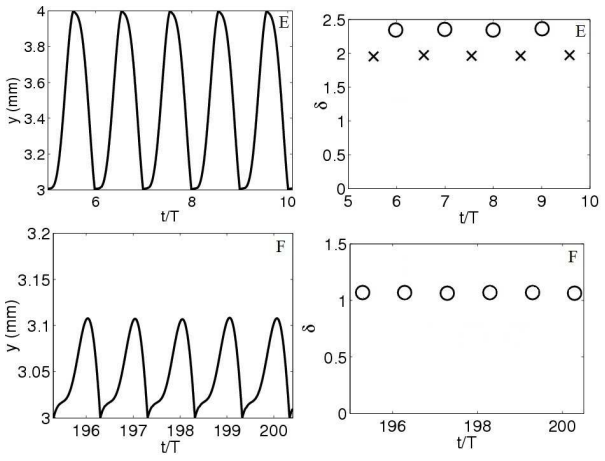

Fig. 5. Vertical coordinate (left column) and SEY impact coefficient (right column) of the effective electron for several points in Fig. 2. SEY coefficient for the impacts with the bottom (upper) wall are denoted by circles (crosses).

IV. Conclusions

In this paper, we have studied the multipactor effect in a ferrite-loaded parallel-plate waveguide. Multipactor simulations made with an in-house code show the multipactor RF voltage threshold in several different scenarios. The effect of the variation of the ferrite magnetization field strength has been considered, finding important deviations from the behavior of the simple metallic parallel-plate structure. In addition, several heights of the ferrite slab have been also considered. Finally, the analysis of some effective electron trajectories reveals the presence of single and double surface multipactor regimes. Thus, it has been found that the apparition of such multipactor modes strongly depends on the ratio between RF frequency and the cyclotron one.

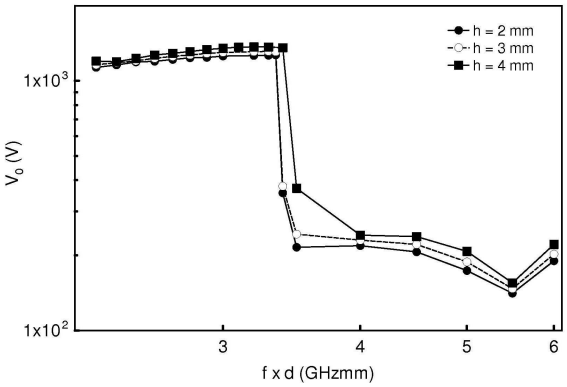

Fig. 6. Multipactor susceptibility charts for silver partially ferrite-filled parallel-plate waveguide. Multipactor voltage threshold for several values of the ferrite slab height. Gap distance is $d = 1$ mm and $H_0 = 1000$ Oe.

REFERENCES

[1] J. Vaughan, "Multipactor", *IEEE Trans. Electron Devices*, Vol. 35, No. 7, pp. 1172-1180, July 1988.

[2] V. E. Semenov, E. I. Rakova, A. G. Sazontov, I. M. Nefedov, V. I. Pozdnyakova I. A. Shereshevski, D. Anderson, M. Lisak, and J. Puech "Simulations of multipactor thresholds in shielded microstrip lines", *Journal of Physics D: Applied Physics*, Vol. 42, Issue 20, article id. 205204, 7 pp., 2009.

[3] A. M. Pérez, C. Tienda, C. Vicente, S. Anza, J. Gil, B. Gimeno, V. E. Boria, "Prediction of Multipactor Breakdown Thresholds in Coaxial Transmission Lines for Traveling, Standing, and Mixed Waves", *IEEE Trans. Plasma Science*, Vol. 37, no. 10, Oct. 2009.

[4] R. Udiljak, D. Anderson, M. Lisak, V. E. Semenov, and J. Puech, "Multipactor in a coaxial transmission line, part I: analytical study", *Phys. Plasmas*, Vol. 14, No. 3, March 2007.

[5] V. E. Semenov, N. Zharova, R. Udiljak, D. Anderson, M. Lisak, and J. Puech "Multipactor in a coaxial transmission line, part II: Particle-in-Cell simulations", *Phys. Plasmas*, Vol. 14, No. 3, March 2007.

[6] C. Vicente, M. Mattes, D. Wolk, B. Mottet, H.L. Hartnagel, J.R. Mosig and D. Raboso, "Multipactor breakdown prediction in rectangular waveguide based components", *Microwave Symposium Digest, 2005 IEEE MTT-S International*, 12-17 June 2005.

[7] C. L. Hogan, "The Ferromagnetic Faraday Effect at Microwave Frequencies and its Applications: The Microwave Gyrator", *Bell System Technical Journal*, vol. 31, no. 1, pp. 1-31, January 1952.

[8] C. E. Fay and R. L. Comstock, "Operation of the Ferrite Junction Circulator", *IEEE Trans. Microwave Theory Tech.*, vol. MTT-13, no. 1, pp.15-27, Jan 1965.

[9] W. J. Ince and E. Stern, "Nonreciprocal remanence phase shifters in rectangular waveguide", *IEEE Trans. Microwave Theory Tech.*, vol. MTT-15, pp. 87-95, Feb. 1967.

[10] W.P. Clark "A High Power Phase Shifter for Phased-Array Systems", *IEEE Trans. Microwave Theory Tech.*, vol. MTT-13, no. 6, pp. 785-788, Nov. 1965.

[11] R. A. Stern, P. Agrios, "A 500 kW X-band Air-Cooled Ferrite Latching Switch", *IEEE Transactions on Microwave Theory and Techniques*, vol. 16, no. 12, pp. 1034-1037, Dec 1968.

[12] J.D. Adam, L.E. Davis, Gerald F. Dionne, E.F. Schloemann, S.N. Stitzer, "Ferrite devices and materials", *IEEE Transactions on Microwave Theory and Techniques*, vol. 50, no. 3, pp. 721-737, Mar 2002.

[13] Ü. Özgür, Y. Alivov, H. Morkoç, "Microwave ferrites, part 2: passive components and electrical tuning", *Journal of Materials Science: Materials in Electronics*, vol. 20, no. 10, pp. 911-952, Oct. 2009.

[14] V. E. Semenov, N. A. Zharova, N. I. Zaitsev, A. K. Gvozdev, A. A. Sorokin, M. Lisak, J. Rasch, and J. Puech, "Reduction of the Multipactor Threshold Due to Electron Cyclotron Resonance", *IEEE Transactions on Plasma Science* vol. 40, no. 11, November 2012.

[15] S. Riyopoulos, D. Chernin, D. Dialetis, "Theory of electron multipactor in crossed fields", *Phys. Plasmas*, vol. 2, no. 8, pp. 3194-3212, 1995.

[16] L. Cai, J. Wang, X. Zhu, Y. Wang, C. Xuan, H. Xia, "Suppression of multipactor discharge on a dielectric surface by an external magnetic field", *Phys. Plasmas*, vol. 18, no. 7, pp. 073504-1 - 073504-6, 2011.

[17] V. E. Semenov, E. Rakova, M. Belhaj, J. Puech, M. Lisak, J. Rasch, E. Laroche, "Preliminary results on the Multipactor effect prediction in RF components with ferrites", *Vacuum Electronics Conference (IVEC), 21-23 May 2013, Paris, IEEE 14th International*.

[18] W. E. Hord "Microwave and millimeter wave ferrite phase shifters", *Microwave Journal* vol. 32, pp. 81-89, 1989.

[19] A. Vegas, A. Prieto, M. A. Solano, "Rigorous analysis of scattering by partial height magnetised ferrite posts in rectangular waveguides", *Electronics Letters*, vol. 18, no. 10, pp. 913-915, May 1992.

[20] A. Abuelma'atti, J. Zafar, I. Khairuddin, A. Gibson, A. Haigh, I. Morgan, "Variable toroidal ferrite phase shifter", *Microwaves, Antennas & Propagation, IET*, vol. 3, no. 2, pp. 242-249, March 2009.

[21] David M. Pozar, "Microwave Engineering", 4th edition, *John Wiley & Sons, Inc.*, 2012.

[22] D. González-Iglesias, M. P. Belloch, O. Monerris, B. Gimeno, V.E. Boria, D. Raboso, V. E. Semenov, "Analysis of multipactor effect using a phase-shift keying single-carrier digital modulated signal", *IEEE Transactions on Electron Devices*, Vol. 60, no. 8, August 2013.

[23] E. Somersalo, P. Yl-Oijala, D. Proch, and J. Sarvas, "Computational methods for analyzing electron multipacting in RF structures", *Part. Accel.*, vol. 59, pp. 107-141, 1998.

[24] S. Anza, C. Vicente, D. Raboso, J. Gil, B. Gimeno, V. E. Boria, "Enhanced Prediction of Multipaction Breakdown in Passive Waveguide Components including Space Charge Effects", *Microwave Symp. Digest, 2008 IEEE MTT-S* pp. 1095-1098.

[25] J. Greenwood "The correct and incorrect generation of a cosine distribution of scattered particles for Monte-Carlo modelling of vacuum systems", *Vacuum* vol. 67, no. 2, pp. 217-222, September 2002.

[26] S. Riyopoulos, "Multipactor saturation due to space-charge-induced debunching", *Phys. Plasmas* vol. 4, no. 5, pp. 14481462, May 1997.

[27] A. Coves, G. Torregrosa-Penalva, C. Vicente, B. Gimeno, and V. E. Boria, "Multipactor discharges in parallel-plate dielectric-loaded waveguides including space-charge effects", *IEEE Trans. on Electron Devices* vol. 55, no. 9, pp. 2505-2511, Sep. 2008.

[28] G. Torregrosa, Ángela Coves, C. Vicente, A. M. Pérez, B. Gimeno, V. E. Boria, "Time Evolution of an Electron Discharge in a Parallel-Plate Dielectric-Loaded Waveguide", *IEEE Electron Device Letters*, Vol. 27, no. 7, July 2006.

[29] I. Montero, F. Caspers, L. Aguilera, L. Galn, D. Raboso, and E. Montesinos, "Low-Secondary Electron Yield of Ferromagnetic Materials and Magnetized Surfaces", *Proc. IPAC'10*, Kyoto, Japan, 23-28 May, 2010.

[30] G. Torregrosa-Penalva, A. Coves, B. G. Martinez, I. Montero, C. Vicente, V. E. Boria,. "Multipactor Susceptibility Charts of a Parallel-Plate Dielectric-Loaded Waveguide", *IEEE Trans. on Electron Devices* vol. 57, no. 5, pp. 1160-1166, May 2010.

[31] R. L. Geng, H. Padamsee, S. Belomestnykh, P. Goudket, D. M. Dykes, R. G. Carter, "Suppression of multipacting in rectangular coupler waveguides", *Nuclear Instruments and Methods Section A*, vol. 508, no. 3, Aug. 2003, pp. 227-238.